A quantitative experimental study of the core excited electronic states of formamide, formic acid, and formyl fluoride

I. Ishii and A. P. Hitchcock
Department of Chemistry, McMaster University, Hamilton, Canada L8S 4M1

(Received 3 February 1987; accepted 2 April 1987)

Optical oscillator strength spectra of formamide ($HCONH_2$), formic acid (HCOOH), and formyl fluoride (HCOF) in the region of K-shell excitation have been derived from electron energy loss spectra recorded under electric dipole dominated scattering conditions (>2.7 keV impact energy, small scattering angle). The observed features are assigned to promotions of 1s electrons to π^*(C=O), σ^*(HCX), σ^*(C–X), σ^*(C=O), and Rydberg orbitals. Systematic changes in the term values for the $1s\rightarrow\pi^*$(C=O) transitions are related to the π donor strengths of the X substituents of the carbonyl group. Broad weak features, observed only in the carbonyl C1s and O1s spectra around 7 eV above the IP, are assigned to $1s\rightarrow\sigma^*$(C=O) transitions. The positions of these features are in agreement with a previously documented correlation with bond length, as are the positions of features associated with σ^*(C–N) in formamide, σ^*(C–O) in formic acid, and σ^*(C–F) in formyl fluoride. The oscillator strengths of the $1s\rightarrow\pi^*$ features in the various K-shell spectra are compared to HAM/3 calculations and are used to estimate the spatial distributions of the π^*(C=O) orbital in the ($1s^{-1}$, π^*) core excited states of these three substituted carbonyl species. We discuss the degree to which these derived orbital maps reflect the spatial distributions of π^*(C=O) orbitals in the ground state.

I. INTRODUCTION

Inner shell electron energy loss spectroscopy (ISEELS) has been used increasingly in recent years to study core-excited electronic states, particularly of molecules containing the second row elements C, N, O, and F.[1,2] ISEELS is well suited for studies of the virtual electronic levels of molecules which contain more than one type of second row atom such as formamide (methamide), formic acid (methanoic acid), and formyl fluoride (monofluoromethanal), since the localization of the core hole allows selective spatial sampling of the optical orbital. The intensities of electronic transitions depend on the symmetry and spatial distribution of the initial and final orbitals. Since the initial orbitals in core excitations are highly localized on a particular atom, the intensities of transitions to the same final orbital from different core levels can be used to map the spatial distribution of the final orbital. In order to use ISEELS for virtual orbital mapping it is necessary to compare intensities in different core spectra and in different molecules. For this purpose we have converted our electron energy loss spectra into absolute optical oscillator strength spectra.

The observed core excitation intensities can be compared to calculated oscillator strengths which in turn can be related to LCAO-MO coefficients if certain approximations are made. In an LCAO description the oscillator strength (f) of an electric dipole core excitation to a nondegenerate state is expressed as[3]:

$$f_{k\sigma} = 0.175 \cdot E \cdot \left| \sum_{h,a} c^{\sigma}_{ha} \langle \chi_{ha} | \mu | \chi_{ks} \rangle \right|^2, \qquad (1)$$

where χ_{ks} is the 1s atomic orbital (C, N, O, or F1s in this study); c^{σ}_{ha} is the coefficient of χ_{ha}, the ath AO function on atom H, in the optical orbital denoted σ; $\mu = e\mathbf{r}$ is the dipole moment operator; E is the transition energy in eV and the matrix element is in units of Å. In this expression terms of the form:

$$|c^{\sigma}_{kp} \langle \chi_{kp} | \mu | \chi_{ks} \rangle|^2$$

are expected to dominate the 1s spectra observed by ISEELS under dipole conditions. The subscript k designates the atom with the 1s core hole while the subscript p refers to np atomic basis functions. The term describing promotions to the 2p orbital on the core excited atom will be the most important since this orbital has the greatest dipole overlap with the 1s orbital. In this series of substituted carbonyls [HCOX (X = NH_2, OH, and F)], the changes of the X substituent are expected to modify the spatial distribution of otherwise similar unoccupied orbitals, such as the π^*(C=O). These changes should be reflected systematically in the 2p LCAO-MO coefficients and thus in the $1s\rightarrow\pi^*$(C=O) intensities. Ideally one wants to compare the experimental oscillator strengths with direct calculations of the transition intensities using Eq. (1). However such information was not available so we have used estimated atomic matrix elements ($\langle \chi_{2p} | \mu | \chi_{1s} \rangle$) to calculate oscillator strengths from HAM/3 LCAO coefficients for the ($1s^{-1}$, π^*) excited states. To our knowledge this is the first application of HAM/3 to core excitation intensities although the application of HAM/3 to calculations of core-excitation energies has been discussed in detail[3] and recently applied to a study of the C1$s\rightarrow\pi^*$ transitions in butadiene.[4] In addition to the comparison at the level of oscillator strengths, we have used the calculated atomic matrix elements to invert our experimental intensities to 2p LCAO coefficients and thus to estimate the spatial distributions of the π^*(C=O) orbital in these molecules. Our experimentally derived coefficients are compared to both excited and ground state calculations which allows us to investigate the influence of the location of

 0021-9606/87/140830-10$02.10

the core hole on the degree of distortion of the π^*(C=O) orbital through relaxation.

Mills and Shirley[5] have used the relative intensities of shake-up transitions in the x-ray photoelectron (XPS) spectrum of formamide to probe orbital spatial distributions. Their results, supported by the theoretical work of Basch,[6] suggested that: (1) the core hole stabilizes the energy of $\pi \rightarrow \pi^*$ valence excitations localized at the core excited atom, and (2) the relative shake-up intensities reflect the density of the π and π^* orbitals on the core excited atom. We find that the trends in the oscillator strengths of $1s \rightarrow \pi^*$ core excitations in formamide are significantly different from those observed[5] in $\pi \rightarrow \pi^*$ valence excitations accompanying core ionization.

The isoelectronic molecules HCOX, where X = NH_2, OH and F, have been studied frequently by means of *ab initio* SCF and CI calculations.[7–10] Changes in the energies and oscillator strengths of the $n \rightarrow \sigma^*$, $n \rightarrow \pi^*$, $\pi \rightarrow \sigma^*$, and $\pi \rightarrow \pi^*$ valence electronic excitations have been discussed in terms of differences in the σ withdrawal and π donation effects of the X substituents. Robin[11] has summarized the theoretical and experimental valence excitation data for these three species. To our knowledge the core excitation spectra of these three species have not been reported previously. The core spectra of acetaldehyde ($HCOCH_3$-ethanal), another member of the HCOX series, has been studied by ISEELS.[12]

II. EXPERIMENTAL

The inner shell electron energy loss spectra were obtained by inelastic scattering of nearly monoenergetic electrons by gases at $\sim 10^{-4}$ Torr with scattering angles of 1°–2°, a final electron energy of 2.5 keV and a resolution of 0.6 eV FWHM. Further details of the technique and the experimental apparatus have been presented elsewhere.[13,14] High purity samples of formamide and formic acid were obtained commercially from Fisher Scientific Co. and BDH Chemicals, respectively. These gases were introduced into the apparatus from the vapors of the room temperature liquids after removing air and volatile impurities by a series of freeze–pump–thaw cycles. Formamide was particularly difficult to study because of its low vapor pressure which required us to bypass the inlet leak valve and introduce the vapor directly into the collision cell through a short tube. Formyl fluoride was synthesized by the fluorination of formic acid, according to literature procedures.[15,16] Briefly, the gases produced from the reaction at 60 °C of an equimolar mixture of formic acid, potassium fluoride, and benzoyl chloride were collected at − 78 °C. The colorless liquid so obtained was purified by vacuum distillation. Since formyl fluoride decomposes in the gas phase over a period of 24 to 48 h at room temperature,[16] the formyl fluoride sample was obtained from the vapor above the purified liquid cooled to − 78 °C in order to retard decomposition. The purity of each sample was monitored *in situ* by quadrupole mass spectrometry. The absolute energy scales were calibrated by recording the spectra of a mixture of the unknown and CO_2.

Formic acid is well known to form dimers by hydrogen bonding. At room temperature the equilibrium saturated vapor pressure of formic acid consists of more than 95% dimers.[17] Dimers are favored at low temperature and high pressure while dissociation into the monomer occurs at reduced pressures or elevated temperatures. At the estimated collision cell pressure of between 10^{-5} and 10^{-4} Torr only 1%–5% of the formic acid molecules will be dimerized at equilibrium.[17] There is a rather convoluted 60 cm path between the low pressure side of our leak valve and the gas cell so that there was ample opportunity for equilibrium to establish through wall collisions. In order to confirm that equilibrium had been established, the gas inlet line on the low pressure side was extended to 4 m. Since there was no significant change in the observed spectra with this modification, we believe that the observed spectra are dominated (>95%) by monomeric formic acid.

III. RESULTS

In order to obtain the approximate optical oscillator strengths from the measured electron energy loss spectra, a small background was first subtracted from each of the spectra in order to remove the contributions from underlying ionization continua. Relative optical spectra were then derived from the background subtracted energy loss spectra by the conversion[18]:

$$\sigma_{\text{opt}}^{\text{rel}} = \sigma_{\text{electron}}^{\text{rel}} / \log[1 + (\theta_m/\theta_E)^2], \tag{2}$$

where the maximum scattering angle, $\theta_m = 2°$, $\theta_E = E/2E_0$, E is the transition energy (energy loss) and $E_0 = E + 2500$ eV for our spectrometer. This operation corrects for differences in the shapes of optical and electron energy loss spectra[18,19] and amounts to a smooth tilt over the 45 eV width of each spectrum ranging from 14% (F1*s*) to 30% (C1*s*). The absolute oscillator strengths were then established by normalization to recent, accurate calculations of atomic oscillator strengths[20] at an energy 25 eV above the IP. At this energy molecular resonance effects are minimal and the oscillator strengths are expected to be atomic like, as has been demonstrated for CO and N_2.[21] The accuracy of this procedure has recently been tested by comparison with a more rigorous full-spectral range sum rule normalization and by comparison with independent measurements of the optical oscillator strengths of N_2, CO, and CO_2.[22] It is well known[19] that there are certain dipole valence excitations whose generalized oscillator strengths are not equal to the corresponding optical oscillator strengths even at quite small momentum transfers. In addition a few nondipole core excitations have been identified[23] under energy loss conditions similar to our experiment. However comparisons indicate that ISEELS in the "dipole regime" and x-ray absorption spectra of the same molecule are generally very similar both as to the transitions excited and their relative intensities. Thus we have chosen this conversion to approximate optical oscillator strengths as a systematic means for comparing intensities among different molecules and among different core edges.

The optical oscillator strength spectra of $HCONH_2$, HCOOH, and HCOF in the region of C1*s* excitation are presented in Fig. 1 while the corresponding O1*s* spectra are shown in Fig. 2. The X1*s* spectra (*K*-shell excitation of the X substituent, i.e., N1*s* in formamide, O1*s* (OH) in formic acid

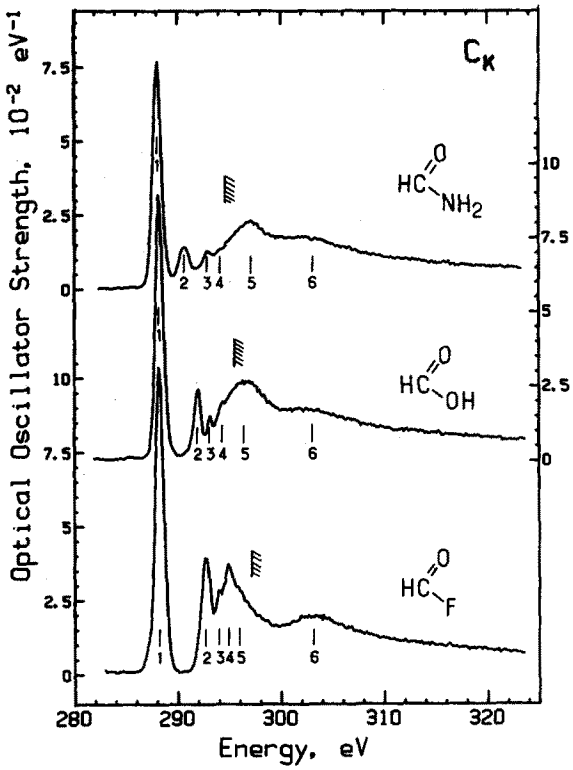

FIG. 1. Optical oscillator strength spectra of formamide, formic acid, and formyl fluoride in the region of C1*s* excitation derived from electron energy loss spectra recorded with 2.5 keV final electron energy, 2° scattering angle and 0.6 eV FWHM resolution.

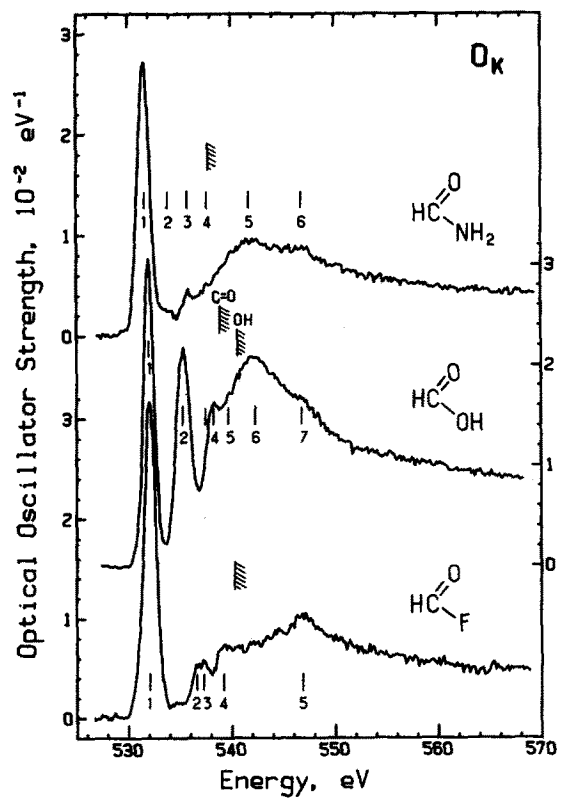

FIG. 2. Optical oscillator strength spectra of formamide, formic acid, and formyl fluoride in the region of O1*s* excitation. See the caption to Fig. 1 for further details.

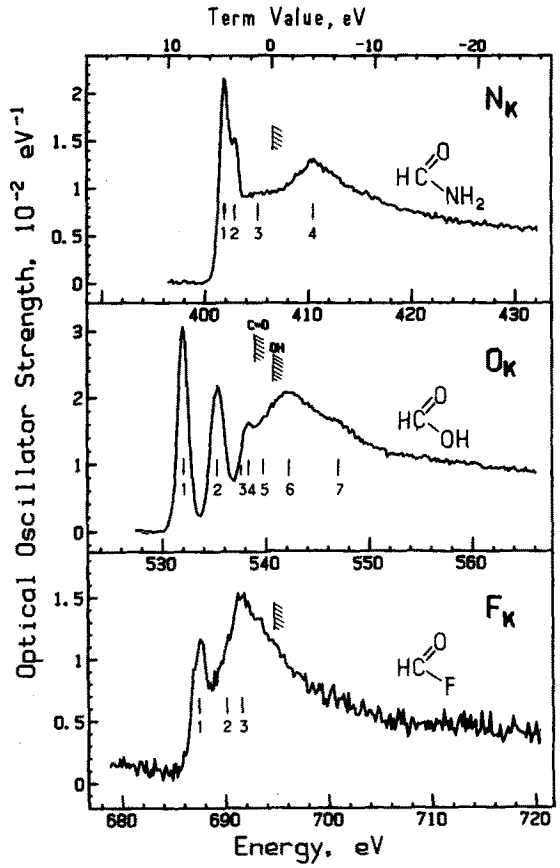

FIG. 3. Optical oscillator strength spectra in the region of substituent X1*s* excitation for formamide (X = nitrogen), formic acid [X = oxygen(OH)], and formyl fluoride (X = fluorine). See the caption to Fig. 1 for further details. The spectra are plotted on a common energy scale relative to the X1*s* IP's.

and F1*s* in formyl fluoride) are shown in Fig. 3, in this case plotted on a common energy scale relative to the substituent ionization potentials (IPs). The core level IPs of formic acid and formamide were taken from XPS.[24] The core IPs of formyl fluoride have not been measured by XPS. The C1*s* and O1*s* IPs are estimated to be 297.1 eV and 540.1 eV, respectively, the average of those of formaldehyde (294.47 for C1*s* and 539.44 eV for O1*s*) and carbonyl fluoride (299.64 for C1*s* and 540.77 eV for O1*s*[24]). The F1*s* IP of HCOF is estimated to be 694.7 eV, 0.7 eV lower than the F1*s* IP of CF_2O (695.43 eV[24]) since the F1*s* IP of CH_3F is 0.73 eV lower than that of CH_2F_2.[24] The energies, term values (T = IP–E) and proposed assignments for the 1*s* excitation features of formamide, formic acid, and formyl fluoride are summarized in Tables I, II, and III, respectively.

The oscillator strengths of individual transitions were measured from these approximate optical spectra by least-squares fits to Gaussian line shapes with the results shown in Fig. 4. From the quality of these fits it is clear that a Gaussian line shape is appropriate. The deviation on the low energy side between the fits and the experimental data for the C1*s* and O1*s* spectra of HCOF probably indicates a small contribution in each spectrum from the intense $1s \rightarrow \pi^*$ transitions in CO, which is a product of the decomposition of HCOF. Table IV summarizes the term values and the derived oscil-

TABLE I. Energies, term values, and proposed assignments for features observed in the K-shell spectra of formamide.

	C1s			O1s			N1s		
#	E ± 0.1 eV	T[a]	#	E ± 0.2 eV	T	#	E ± 0.2 eV	T	Assignment final orbital
1[b]	288.1	6.4	1	531.5	6.0	1	401.9	4.6	π^*(C═O)
2	290.7	3.8	2	533.8	3.9	2	402.9	3.6	3s/σ^*(HCN)
3	292.9	1.6	3	535.9	1.8	3	405(1)	1.5	3p
4	294.1	0.4	4	537.7	0		···		higher Rydberg
IP[c]	294.5			537.7			406.5		
5	296.9	−2.4	5	541.8	−4.1	4	410.5	−4.5	σ^*(C–N)
6	303(1)	−8.5	6	547(1)	−9.3		···		σ^*(C═O)

[a] $T = \mathrm{IP} - E$.
[b] Calibration: C1s[2.67(5) eV below π^* in CO_2 [290.74(5) eV (Ref. 36)]}, O1s [129.6(1) eV above N1s→π^*(C═O) in $HCONH_2$]. N1s [113.8(1) eV above C1s→π^*(C═O) in $HCONH_2$].
[c] From XPS (Ref. 24).

TABLE II. Energies, term values, and proposed assignments for features observed in the K-shell spectra of formic acid.

	C1s			O1s(C═O)			O1s(C–OH)		
#	E ± 0.1 eV	T	#	E ± 0.2 eV	T[a]	#	E ± 0.2 eV	T[a]	Assignment final orbital
1[b]	288.2	7.6	1[b]	532.1	6.9	2	535.3	5.4	π^*(C═O)
2	292.0	3.8	2	535.3	3.7		···		3s/σ^*(HCO)
3	293.2	2.6		···		4	538.3	2.4	3p
4	294.2	1.6	3	537.6	1.4	5	539.6	1.1	higher Rydberg
IP[c]	295.8			539.0			540.7		
5	296.1	−0.3		···		6	542.1(5)	−1.4	σ^*(C–OH)
6	303(1)	−7.2	7	547(1)	−8		···		σ^*(C═O)

[a] $T = \mathrm{IP} - E$. The appropriate O1s IP is used in the case of the O1s features.
[b] Calibration: C1s {1.55(5) eV below π^* in CO_2 [290.74(5) eV (Ref. 36)]}, O1s {3.30(9) eV below π^* in CO_2 [535.4(1) eV (Ref. 37)]}.
[c] From XPS (Ref. 24).

TABLE III. Energies, term values, and proposed assignments for features observed in the K-shell spectra of formyl fluoride.

	C1s			O1s			F1s		
#	E ± 0.1 eV	T	#	E ± 0.2 eV	T	#	E ± 0.3 eV	T	Assignment final orbital
1[a]	288.2	8.9	1	532.1	8.0	1	687.7	7.0	π^*(C═O)
2	292.7	4.3	2	536.6	3.5	2	690.5(5)	4.2	3s/σ^*(HCF)
3	294.0	3.1	···	···	3p				
4	294.9	2.2	3	537.6	2.5	3	691.5	3.2	σ^*(C–F)
5	296.0	1.1	4	539.2	0.9	···	4p		
IP[b]	297.1(3)			540.1(3)			694.7(4)		
6	303(1)	−6	5	547(1)	−7		···		σ^*(C═O)

[a] Calibration: C1s {2.53(5) eV below π^* in CO_2 [290.74(5) eV (Ref. 36)]}, O1s {3.30(9) eV below π^* in CO_2 [535.4(1) eV (Ref. 37)]}, F1s [155.6(1) eV above O1s→π^*(C═O) in HCOF].
[b] Estimated from the XPS IPs of CH_2O, CF_2O, CH_2F_2, and CH_3F (Ref. 24)—see the text.

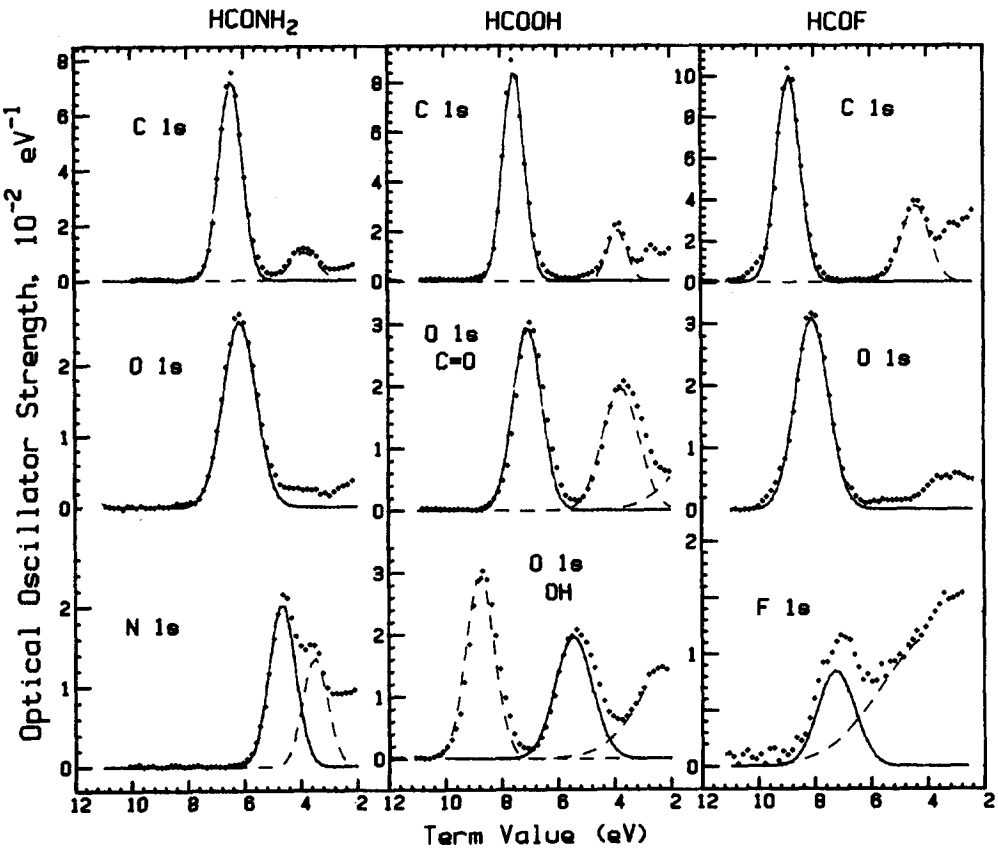

FIG. 4. Least-square fits of Gaussian line shapes and a linear background to the $1s\rightarrow\pi^*$ region of each spectrum. Where necessary a second peak representing higher energy transitions has been added to obtain an adequate fit.

lator strengths for all $1s\rightarrow\pi^*$ transitions in comparison to the corresponding quantities obtained or derived from HAM/3 core excitation calculations. The intensities are discussed in Sec. IV A 2 following interpretation of the trends in the π^* term values.

IV. DISCUSSION

A. $1s\rightarrow\pi^*$(C=O) transitions

1. Term values

The C1s and O1s spectra of all carbonyl species (H_2CO, CH_3CHO, $(CH_3)_2CO$,[12] F_2CO, $(CF_3)_2CO$[25] exhibit sharp, intense $1s\rightarrow\pi^*$(C=O) features with term values (T = IP–E) between 6 and 10 eV. Similarly, intense $1s\rightarrow\pi^*$(C=O) features occur in both the C1s and O1s spectra of the molecules studied in this work. The term values of the $C1s\rightarrow\pi^*$(C=O) transitions [$T(C1s^{-1},\pi^*)$] in the HCOX species increase systematically with the increasing electronegativity of the X substituent from 6.4 in formamide to 8.9 eV in formyl fluoride. $T(O1s^{-1},\pi^*)$ also changes from molecule to molecule. In each species it is slightly lower than the corresponding $T(C1s^{-1},\pi^*)$. Although none of the features in the C1s spectra of acetaldehyde or acetone[12] were attributed to $C1s(CH_3)\rightarrow\pi^*$(C=O) transitions, prominent $X1s\rightarrow\pi^*$ transitions are observed in the three molecules of the present study. The $X1s\rightarrow\pi^*$ transition is the first feature in the N1s spectrum of $HCONH_2$ and in the F1s spectrum of HCOF. The second feature in the O1s spectrum of formic acid is assigned primarily to $O1s(OH)\rightarrow\pi^*$(C=O) transitions, although it probably also contains contributions from excitations of the carbonyl oxygen [O1s(C=O)] to another excited level. Over the HCOX series $T(X1s^{-1},\pi^*)$ increases by 2.4 eV, parallel to the trends in $T(C1s^{-1},\pi^*)$ and $T(O1s^{-1},\pi^*)$.

These results show that the energies of the $\{1s^{-1},\pi^*(C{=}O)\}$ excited states change systematically with the location of the core hole as well as with the electronegativity of the substituents. Within each molecule, $T(C1s^{-1},\pi^*)$ is 0.4 to 0.9 eV larger than $T(O1s^{-1},\pi^*)$ and almost 2 eV larger than $T(X1s^{-1},\pi^*)$. If one assumes that the shifts in

TABLE IV. Experimental and HAM/3 calculated term values (T, eV) and oscillator strengths (f, 10^{-2}) for the $1s\rightarrow\pi^*$(C=O) transitions in formamide, formic acid, and formyl fluoride.

	C1s	O1s	X1s
	T(f, 10^{-2})	T(f, 10^{-2})	T(f, 10^{-2})
$HCONH_2$ exp.[a]	6.4(7.4)	6.0(3.8)	4.6(2.3)
HAM/3[b]	5.6(16.2)	4.9(4.8)	3.9(2.3)
HCOOH exp.	7.6(8.0)	6.9(3.7)	5.4[3.2][c]
HAM/3	6.7(17.4)	5.8(4.7)	4.7(1.7)
HCOF exp.	8.9(10.4)	8.0(4.5)	7.0(1.4)
HAM/3	8.0(18.0)	6.8(5.8)	5.7(0.7)

[a] Peak area calculated by least-squares Gaussian fitting to each π^* peak (see Fig. 4).

[b] Term values predicted from HAM/3 calculations of the $1s\rightarrow\pi^*$ states using a transition state procedure. The oscillator strengths were derived from the HAM/3 2p LCAO coefficients and calculated atomic matrix elements, as discussed in the text.

[c] This is probably significantly larger than the true intensity of the $O1s(OH)\rightarrow\pi^*$ transition because of overlap with the $O1s(C{=}O)\rightarrow 3s/\sigma^*(HCX)$ feature.

term values with core hole location reflect the relative strength of the attraction between the excited electron and the core hole, the term value shifts are consistent with the spatial distributions of the excited electron in the π^*(C=O) orbital (see Sec. IV A 2). According to the π^* spatial distribution, derived from the ISEELS intensities or calculations, the overlap will be greatest and thus the term value largest (attraction strongest) when the core hole is on the carbonyl carbon atom, somewhat weaker when the core hole is on the carbonyl oxygen atom and weaker still when the core hole is on the substituent atom.

When comparing among molecules, the π^*(C=O) orbital becomes more tightly bound (i.e., $T(1s^{-1},\pi^*)$ is larger) as the substituent electronegativity increases. This shift can be explained in terms of either decreasing π donor strength[11] or increasing charge withdrawal via the σ orbitals. The π-donor strength of N is greater than that of O or F at least in part because of the better match between N2p and C2p/O2p AO energies. Decreased π donation results in less π delocalization and thus a smaller π-π^* splitting and larger π^* term value, as observed. In principle charge withdrawal from the carbonyl onto the X substituent will increase the effective nuclear charge felt by an electron primarily located on the carbonyl group and thus can increase the π^*(C=O) orbital binding energies. However σ charge withdrawal is a very minor factor in determining the π^* energy as demonstrated by the fact that the term value for C1s→π^* transitions is essentially constant through each of the series of fluorobenzenes, $C_6H_xF_{6-x}$, $x=0$–6,[26] fluoroethenes, $C_2H_xF_{4-x}$, $x=0$–4[22] and fluorocarbonyls, $H_xF_{2-x}C{=}O$, $x=0$–2.[12,25] It would appear that the local dipole associated with a C–F bond is not effective in modifying the π interactions when it is perpendicular to the 2p orbitals of the π system.

The π^* orbital energies determined from HAM/3 transition state calculations of the $(1s^{-1},\pi^*)$ states are compared to the experimental term values in Table IV. The calculated values match the experimental results remarkably well although there is a displacement to lower term value (thus higher predicted transition energy) of 0.9 eV for C1s, 1.1 eV for O1s(C=O) and 0.7–1.3 eV for X1s. HAM/3 calculations of core excitation term values are consistently lower than the observed values.[3]

2. Oscillator strengths

In addition to the term values, the intensities of the 1s→π^* transitions change systematically, both in the same molecule, with the location of the core hole and between molecules, as the electronegativity of the substituent changes. In each molecule, the C1s→π^*(C=O) transitions are the most intense, the O1s→π^*(C=O) transitions slightly weaker and the X1s→π^*(C=O) transitions much weaker. This indicates that the π^*(C=O) electron is localized more at the carbon than at the oxygen of the carbonyl group and has relatively little density at the substituent atom. Among the three HCOX molecules, the intensity of the C1s→π^*(C=O) feature increases with increasing substituent electronegativity. In contrast, the intensity of the O1s→π^*(C=O) feature is similar in all three species. The X1s→π^*(C=O) transition in $HCONH_2$ is more intense than that in HCOF while the O1s(OH)→π^*(C=O) transition in HCOOH is apparently the most intense of the three. We interpret the anomalously large intensity of the O1s(OH)→π^*(C=O) feature in HCOOH to contributions by transitions from O1s(C=O) to another excited level. We note that the X1s→π^* intensities are the least accurate because of peak overlap in the N1s ($HCONH_2$) and O1s (HCOOH) spectra and the somewhat poorer statistics of the F1s spectrum of HCOF. Extrapolation of the trend of X1s→π^*(C=O) intensities in this series would predict a relatively strong C1s(CH_3)→π^* transition in CH_3CHO. A feature corresponding to such a transition was not identified in the original interpretation of the C1s spectrum of acetaldehyde[12] although a possible candidate is a weak shoulder at 287.2 eV ($T=4.0$ eV) which was assigned to C1s→4s Rydberg transitions (see Fig. 5 of Ref. 12). If this is the corresponding C1s(CH_3)→π^* transition it is certainly anomalously weak compared to the trend in the intensities of the X1s→π^* transitions in the present series. This suggests that it is necessary to have substituent lone pairs in order to have appreciable π^* density at the substituent atom. The delocalization of π^*(C=O) onto the CH_3 group in acetaldehyde can also be discussed in terms of mixing of the $e(\pi)$ component of the CH_3 group orbitals in the π^*(C=O) orbital—an effect mixing known as hyperconjugation. Hyperconjugation is known to be weaker than the mixing of the C 2p and O 2p orbitals with the X 2p "lone pair" orbitals in the π manifold of formamide, formic acid, and formyl fluoride.

Oscillator strengths have been calculated from HAM/3 C2p LCAO coefficients in the $(1s^{-1},\pi^*)$ states by means of the approximate formula:

$$f=0.175\cdot E\cdot c_{2p}^2\,|\langle\chi_{2p}|\mu|\chi_{1s}\rangle|^2. \tag{3}$$

The atomic matrix elements were estimated from HAM/3 Slater orbital (STO) exponents (using the ground state value for the core orbital and the excited state value for the optical 2p orbital) and an analytical formula for STO integrals given by McGlynn *et al.*[27] For formamide this calculation gives matrix elements of 0.0860 Å (C1s→C2p), 0.0718 Å (N1s→N2p) and 0.0602 Å (O1s→O2p). The decrease in the matrix element with increasing transition energy primarily reflects the contraction of the orbital radii with increasing Z. To first order the atomic $\langle\chi_{2p}|\mu|\chi_{1s}\rangle$ matrix elements will vary as Z^{-1}. The product of Z and the matrix element is 0.52, 0.50, and 0.48, respectively, for C1s, N1s, and O1s.

The 1s→π^* oscillator strengths calculated from the 2p coefficients in the HAM/3 excited states and these atomic matrix elements are compared to the experimental results in Table IV. Experiment and theory agree within a factor of 3 in all cases. This seems remarkable given the numerous approximations made in obtaining both the experimental and calculated oscillator strengths. The average ratio of the calculated to the experimental intensities is 2.0 for C1s→π^*, 1.2 for O1s→π^*, and 0.6 for X1s→π^* transitions. In general HAM/3 and other one-electron calculations of electronic transition intensities are larger than experimental values by roughly a factor of 2.[3] Thus the C1s and O1s results appear consistent with previous experience whereas the X1s→π^*

transitions are considerably stronger than expected from the calculations.

The spatial distributions of the π^*(C=O) orbitals in $HCONH_2$, HCOOH, and HCOF in the form of squared $2p$ coefficients calculated from Eq. (3) using the estimated atomic matrix elements and the experimental oscillator strengths are listed in Table V and presented graphically in Fig. 5, in comparison to the HAM/3 squared $2p$ coefficients of the π^* orbital in the ($C1s^{-1}$,π^*) states. In general there is remarkably good agreement between the experimentally derived and calculated π^* spatial distributions although the experimental results suggest that there is relatively greater density on the oxygen and substituent atoms than predicted by the calculations, particularly when the predeliction for overestimation in the calculation is taken into account.

If core hole relaxation effects are small these experimentally derived c_{2p}^2 values should reflect the spatial distribution of the π^*(C=O) orbital in the ground state. The validity of this approximation can be investigated by comparing values derived from the core excitation intensities with calculated $2p$ LCAO-MO coefficients of the π^* orbital in the *ground state*. The results of three different ground state calculations[7,28] are also listed in Table V. According to all ground state calculations, the C$2p$ LCAO coefficients of the π^* orbital stay nearly constant or slightly decrease in the order $NH_2 > OH > F$. This trend is opposite to that of the observed oscillator strengths of the C$1s \rightarrow \pi^*$(C=O) features. On the other hand the HAM/3 calculation of core excitation reverses this trend and predicts that the π^* orbital becomes more concentrated on the carbon atom as the X electronegativity increases. The carbonyl O$2p$ LCAO coefficients are approximately the same from molecule to molecule, a trend which agrees with the coefficients derived from the core excitation oscillator strengths. According to both the ground and core excited state calculations the density of the π^* orbital on the substituent atom is much smaller than on the carbon or oxygen atoms of the carbonyl whereas the coefficients derived from the ISEELS intensities suggest a relatively larger contribution of the X$2p$ AO to the π^* MO. It is probable that at least part of the surprisingly strong X$1s \rightarrow \pi^*$ intensity is an effect of relaxation and the distortion of the π^* electron distribution towards the core hole. The F$1s \rightarrow \pi^*$ transition of HCOF is surprisingly intense and has the greatest discrepancy with the calculations. Thus it would appear that the core hole distortion of the π^* orbital is strongest in HCOF. It is possible that, in the other X substituents, the hydrogen atoms provide enough electron density to shield the X$1s$ core hole so that the intrinsic π^*(C=O) density is not drastically affected by the N$1s$ ($HCONH_2$) or O$1s$ (HCOOH) core holes. The absence of distortion of the π^*(C=O) electron distribution towards the core hole in the C$1s$(CH_3^{-1},π^*) states of $HCOCH_3$ probably explains why the C$1s$(CH_3)$\rightarrow\pi^*$(C=O) transitions in CH_3CHO and $(CH_3)_2CO$ are weak or absent.

The aforementioned discrepancies between experiment and ground state calculations, in the trends at carbon with changing electronegativity, and in the relative C/O/X contributions, could be interpreted solely as the influence of the core hole. However the HAM/3 transition state calculation of the core excitation, which should account for the changes in the π^* distribution caused by the core hole, shows most of the same discrepancies with experiment as do the ground state calculations. It is possible that the discrepancies

TABLE V. Squares of calculated and derived $2p$ LCAO coefficients of the π^* orbital of formamide, formic acid, and formyl fluoride.

Excited atom	Core excited state		Ground state		
	exp.[a]	HAM/3[b]	HAM/3	(Ref. 28)[c]	(Ref. 7)[c]
$HCONH_2$					
C	0.20	0.43	0.58	0.74	0.76
O	0.11	0.13	0.28	0.30	0.29
N	0.06	0.07	0.14	···	0.18
HCOOH					
C	0.21	0.46	0.61	0.72	0.59
O(C=O)	0.11	0.14	0.29	0.34	0.27
O(OH)	[0.06][d]	0.05	0.11	···	0.10
HCOF					
C	0.28	0.48	0.61	0.69	0.50
O	0.13	0.17	0.31	0.40	0.28
F	0.06	0.03	0.07	···	0.05

[a] Derived from Eq. (3) using the experimental oscillator strengths (Table IV), transition energies and the following calculated atomic $\langle\chi_{2p}|\mu|\chi_{1s}\rangle$ matrix elements (Ref. 27): C$1s$ (0.086^2), N$1s$ (0.072^2), O$1s$ (0.060^2), F$1s$ (0.044^2).

[b] These coefficients do not sum to unity because they are taken from calculations of different ($1s^{-1}$, π^*) states which are thus normalized differently.

[c] Only the square of the coefficient of the more compact function of these double zeta basis functions was used to calculate c_{2p}^2 as this will have greater overlap with the core.

[d] Based on an estimated oscillator strength of 0.020 for the O$1s$(OH)$\rightarrow\pi^*$ component of feature 2 in the O$1s$ spectrum of HCOOH.

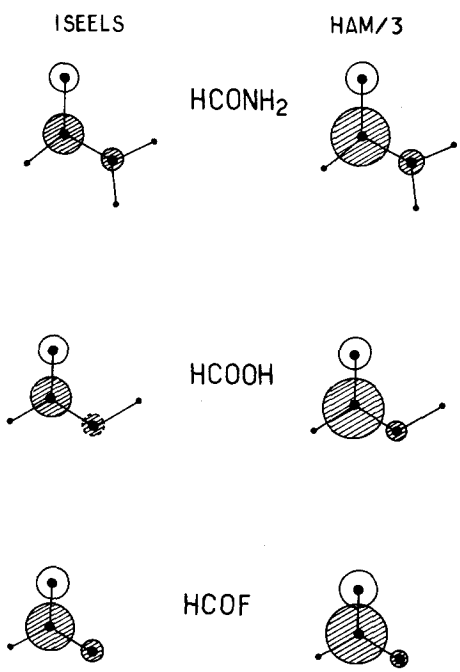

FIG. 5. Sketches of the spatial distributions of the π^*(C=O) orbitals based on (a) the $2p$ LCAO coefficients obtained from the optical oscillator strengths corrected by the transition energy and estimated $\langle\chi_{2p}|\mu|\chi_{1s}\rangle$ atomic matrix elements and (b) the $2p$ LCAO coefficients from HAM/3 calculations of the $1s$ excitation. The areas of each circle are proportional to the squared $2p$ coefficient.

between the calculated and experimental intensities reflect the limitations of the calculations rather than solely distortions of the π^* orbital by the core hole. If this is so the possibility remains that the core excitation intensities can be used to map ground state virtual orbitals. One factor that we have neglected is contributions to the oscillator strength from matrix elements involving is overlap with other AO components of the π^* orbital, such as higher *np* orbitals on the core excited atom or 2*p* orbitals on neighboring atoms. A more complete calculation of core excitation intensities is required to estimate the importance of these terms.

The $1s \rightarrow \pi^*$ intensities at different core edges in formamide are considerably different from the oscillator strengths of the $\pi \rightarrow \pi^*$ shake-up lines in XPS.[4] In particular the ISEELS pattern $[I_C > I_O \gg I_N]$, which we interpret to reflect the π^* spatial distribution, is different from that of $[I_O \sim I_C \gg I_N]$ for the $\pi_1 \rightarrow \pi_3^*$ shake up, or that of $[I_O \gg I_N > I_C]$ for the $\pi_2 \rightarrow \pi_3^*$ shake up. As explained by Mills and Shirley,[4] the shake-up intensities reflect the spatial distributions of *both* the unoccupied π^* and the occupied π orbitals. It would appear that, although both XPS shake-up and core excitation are useful probes of orbital spatial distributions because of the localized core hole in each spectroscopy, core excitation is intrinsically simpler to interpret since it generally involves only one other orbital. In addition ISEELS intensities are much greater than XPS shake-up intensities and thus easier to measure experimentally.

B. $1s \rightarrow 3s/\sigma^*$(HCX) transitions

In the C1*s* spectra of all three species (Fig. 1) a second feature of moderate intensity is observed with term values (oscillator strengths) of 3.8 eV (0.013), 3.8 eV (0.018), and 4.3 eV (0.046) for formamide, formic acid, and formyl fluoride, respectively. The oscillator strength of this feature increases appreciably from $HCONH_2$ to HCOF. Although the term values of these features are consistent with an assignment to $C1s \rightarrow 3s$ Rydberg transitions, the variable intensity suggests that the excited states do not have solely Rydberg character since the intensities of corresponding Rydberg excitations are expected to be similar in molecules of similar size, or possibly to decrease as the substituent electronegativity increases if there are potential barrier effects.[29] Further evidence that these features have a significant valence character comes from the spectrum of solid formic acid,[30] which shows a relatively strong feature at essentially the same energy. Weak features with similar term values (3.4, 3.7, and 3.1 eV) are observed in the O1*s*(C=O) spectra (Fig. 2). In the X1*s* spectra (Fig. 3), the second feature is observed as a prominent peak overlapping the high energy side of the $N1s \rightarrow \pi^*$ transition of formamide, while in formic acid the corresponding O1*s*(OH) excitation probably blends with the high energy side of feature 2 and cannot be identified. Although the statistics of the F1*s* spectrum of HCOF are somewhat limited there appears to be a shoulder around 690.5 eV which may be the corresponding feature. In contrast to the $C1s \rightarrow \pi^*$(C=O) transitions, the term value of the second C1*s* feature increases only slightly with increasing substituent electronegativity. From the weak O1*s* intensity and the moderately large C1*s* and X1*s* intensities of these features, it appears that the final orbital of this transition is localized on the C and X atoms.

In the UV spectra of all amides a relatively weak band is observed about 1 eV below the singlet–singlet $\pi \rightarrow \pi^*$ band. Based on all-electron GTO-SCF calculations,[11,31] an $n \rightarrow \sigma^*$ excitation has been suggested for this feature. The calculations show that the terminating level is a σ orbital involving C and N AOs. Analogous features have been observed in the valence excitation spectra of olefin compounds where they have been assigned to $\pi \rightarrow \sigma^*$(C–H) transitions.[32,33] The second optical orbital in formaldehyde is calculated to have a $\sigma^*(CH_2)$ character,[7] analogous to the $\sigma^*(CH_2)$ orbital in ethene.[7,34] In carbonyl fluoride the second optical orbital is centered at the fluorine and carbon atoms, according to the ground state calculations.[7] Since formyl fluoride is intermediate between formaldehyde and carbonyl fluoride, a similar σ^* orbital may be expected. The above considerations are the origin of our proposed σ^*(HCX) designation for the upper orbital of the second transition in the HCOX series. Low-lying orbitals of σ^*(HCX) character can be identified in the ground state calculations[7,34] of all three HCOX molecules. Based on the assignment of the valence spectra of olefins and amides and the calculations,[7,31,34] we propose that the second feature in each spectrum arises from 1*s* excitations to an orbital of mixed 3*s* Rydberg/σ^*(HCX) valence character.

C. Other $1s \rightarrow$ Rydberg transitions

The degree of Rydberg or valence character of the states observed between the first $1s \rightarrow \pi^*$(C=O) transition and the IP is an interesting question. Core-excited Rydberg states have been identified in the past generally on the basis of characterisic term values which are around 3.5–4.5 eV, 2.4–3.2 eV, and 1.6 eV, respectively, for the lowest energy *s*, *p*, and *d* Rydberg states (corresponding to quantum defects around 1, 0.6, and 0.1, respectively[11]). In addition Rydberg excitations are usually (but not always) weaker and sharper than valence excitations. Feature 3 in the C1*s* spectrum of formyl fluoride, with a term value of 3.1 eV is attributed to $C1s \rightarrow 3p$ transitions. Feature 3 in the C1*s* spectrum of formic acid ($T = 2.6$ eV) is also a good candidate for a 3*p* Rydberg transition. We assign the $C1s \rightarrow 3p$ transition in formamide to feature 3, although it appears to have an anomalously low term value ($T = 1.6$ eV). These $(C1s^{-1},3p)$ states are thought to be relatively pure Rydberg ones, in contrast to the virtual valence description we have emphasized in the preceding discussion of the $3s/\sigma^*$(HCX) features. Other weak features in these spectra have been identified as Rydberg transitions on the basis of their term values as outlined in Tables I–III. We expect that higher resolution core excitation spectra of these molecules will differ from the present results primarily in the detection of further Rydberg features. In general the Rydberg transitions are most intense in the C1*s* spectra and relatively weak in the O1*s* and X1*s* spectra. This effect has been noted in previous work on core excitation.[12] It may be the result of the somewhat greater extent of the C1*s* AO which results in better overlap with the spatially extended Rydberg orbitals.

TABLE VI. Predicted and observed positions of the σ^*(C=O) and σ^*(C–X) shape resonances of formamide (X = N), formic acid (X = O), and formyl fluoride (X = F).

		σ^*(C–X) δ^b (eV)					σ^*(C=O) δ^b (eV)			
	R(Å)[a]		Obs.			R(Å)[a]		Obs.		
Molecule	(C–X)	Pred.	Avg.	C	X	(C=O)	Pred.	Avg.	C	O
$HCONH_2$	1.368	3.9	3.4	2.4	4.5	1.219	6.7	8.9	8.5	9.3
HCOOH	1.358	2.6	0.8	0.3	1.4	1.214	6.8	7.6	7.2	8.0
$(HCOOH)_2$	1.320	3.7				1.217	6.7			
HCOF	1.338	−2.7	−2.2	−2.2	−3.2	1.181	7.8	6.5	6	7

[a] Reference 35.

[b] $\delta_\sigma = E_\sigma$–IP($= -T$). The predicted values have been calculated from the least-squares correlation lines presented in (Ref. 2).

D. σ^*(C–X) and σ^*(C=O) transitions: bond length correlations

A broad peak occurs above the C1s IP in $HCONH_2$, at the C1s IP in HCOOH and just below the C1s IP in HCOF. Corresponding broad features are observed at similar term values in the X1s spectra and very weakly in the O1s(C=O) spectra. These features are assigned to $1s \rightarrow \sigma^*$(C–X) excitations. The relative intensities in the various K-shell spectra suggest that these orbitals are localized mainly between the carbon and X atoms, consistent with our σ^*(C–X) assignment. In addition the average term values are in good agreement with the predictions of the bond length correlation[2] and the known C–X bond lengths[35] (see below).

In the C1s spectra of all three species a broad weak peak (#6) is observed around 6–8 eV above the IP. Features with similar shape and term values are also observed in the O1s(C=O) spectra but not in any of the X1s spectra. These features are assigned to σ^*(C=O) shape resonances (transitions to a quasibound σ^*(C=O) orbital). Similar features are observed in the K-shell spectra of formaldehyde, acetaldehyde and acetone[12] and in F_2CO, $(CF_3)_2CO$, and CF_3CO_2H[25] and thus appear to be characteristic of the carbonyl group.

The positions of the σ^*(C–X) and σ^*(C=O) resonances in this series of molecules may be compared with the values predicted from the empirical bond length correlation.[2] The observed and predicted resonance energies relative to the IP, $\delta = E - \text{IP} = -T$, are summarized in Table VI along with the predicted δ values for the σ^*(C–X) and σ^*(C=O) resonances in the formic acid dimer. As in previous work[2] the δ values of $1s \rightarrow \sigma^*$ transitions in the core spectra of the atoms at each end of the bond are similar and thus these have been averaged for comparison with the predictions of the correlation, which was generated from similarly averaged data. For the σ^*(C=O) resonances the $Z = 14$ correlation line[2] predicts δ values between 6.7 and 7.8 eV based on the carbonyl bond lengths which vary systematically from 1.219(12) Å in formamide to 1.181(5) Å in formyl fluoride.[35] The maxima of the broad σ^*(C=O) resonances occur between 6.5 and 8.9 eV. Considering the uncertainty in determining the positions of the broad resonances and the scatter in the correlation,[2] the agreement between the predicted and observed $1s \rightarrow \sigma^*$(C=O) positions appears reasonable.

In order to correlate the positions of $1s \rightarrow \sigma^*$(C–X) transitions with the C–X bond lengths the Z dependence of the σ resonance position must be taken into account. Thus although the C–X bond lengths are very similar in these three molecules, the σ^*(C–X) resonance positions vary significantly from molecule to molecule because of the Z dependence. There is reasonable agreement between the observed and predicted σ^*(C–X) values (Table VI), supporting our assignments.

V. CONCLUSIONS

The optical oscillator strengths of the isoelectronic series of molecules, formamide, formic acid, and formyl fluoride have been derived from inner shell electron energy loss spectra, all for the first time to our knowledge. The oscillator strengths of transitions to the same final level from all atomic K shells, as well as trends in the term values, have provided the basis for our assignments of the observed features. The oscillator strengths and term values of the $1s \rightarrow \pi^*$(C=O) transitions vary systematically with the electronegativity of the X substituent in the HCOX series. Changes in the $1s \rightarrow \pi^*$ term values have been rationalized in terms of the relative π-donor strength of the substituents. The experimental intensities have been used to map the spatial distribution of the π^* orbital in each molecule. The $X1s \rightarrow \pi^*$ transitions are found to be surprisingly intense, suggesting that the π delocalization of these molecules is greater than previously believed although distortion of the π^* orbital by the X1s core hole is an alternate explanation.

Features in the carbon and substituent 1s spectra around the IP are assigned to $1s \rightarrow \sigma^*$(C–X) transitions while weak, broad features around 303 eV, which appear only in the C1s and O1s continua, are assigned to σ^*(C=O) resonances. The positions of both the σ^*(C–X) and σ^*(C=O) resonances are in agreement with the values predicted from the bond length correlation.[2]

Finally we wish to emphasize that the ability to obtain the spectra of a reactive, relatively short-lived species such as HCOF indicates that core excitation in general and ISEELS in particular is an attractive technique for studying the optical orbitals of transient molecular species. An advantage of ISEELS over other popular, complementary spectroscopies of short-lived molecules such as PES is the ability to carry

out semiquantitative elemental analysis on the gas present in the collision cell simply by recording a wide energy range spectrum.

ACKNOWLEDGMENTS

We thank Professor E. Lindholm for performing the HAM/3 calculations, the matrix element estimates and for many helpful discussions. We also thank Dr. W. H. E. Schwarz and R. McLaren for their critical readings of the manuscript and Dr. P. Millie for helpful comments. This research has been supported financially by the Natural Sciences and Engineering Research Council of Canada (NSERC). APH gratefully acknowledges the support of an NSERC university research fellowship and the hospitality of LURE, where this manuscript was written during a research leave.

[1]C. E. Brion, S. Daviel, R. N. S. Sodhi, and A. P. Hitchcock, AIP Conference Proceedings **94**, 426 (1982); A. P. Hitchcock, J. Electron Spectrosc. **25**, 245 (1982).
[2]F. Sette, J. Stöhr, and A. P. Hitchcock, J. Chem. Phys. **81**, 4906 (1984).
[3]E. Lindholm and L. Åsbrink, *Molecular Orbitals and their Energies, Studied by the Semiempirical HAM Method* (Springer, Berlin, 1985), p. 150.
[4]E. Lindholm, J. Chem. Phys. **85**, 1484 (1986).
[5]B. E. Mills and D. A. Shirley, Chem. Phys. Lett. **39**, 236 (1976).
[6]H. Basch, Chem. Phys. Lett. **37**, 447 (1976).
[7]L. C. Snyder and H. Basch, *Molecular Wavefunctions and Properties* (Wiley, New York, 1972).
[8]J. E. Del Bene, G. T. Worth, F. T. Marchese, and M. E. Conrad, Theor. Acta Berlin **36**, 195 (1975).
[9]S. D. Peyerhimhoff and R. J. Buenker, J. Chem. Phys. **50**, 1846 (1969); N. L. Allinger, M. J. Sister, and M. J. Hickey, Tetrahedron **28**, 2157 (1972).
[10]L. Z. Stenkamp and E. R. Davidson, Theor. Chim. Acta Berlin **44**, 405 (1977); E. Oliveros, M. Riviere, C. Teichteil, and J. P. Malrieu, Chem. Phys. Lett. **57**, 220 (1978); L. B. Harding and W. A. Goddard III, J. Am. Chem. Soc. **97**, 6300 (1975); E. Lindholm, G. Bieri, L. Åsbrink, and C. Fridh, Int. J. Quantum Chem. **14**, 737 (1978).
[11]M. B. Robin, *Higher Excited States of Polyatomic Molecules*, Vol. 2 (Academic, New York, 1974); Vol. 3 (1985).
[12]A. P. Hitchcock and C. E. Brion, J. Electron Spectrosc. Relat. Phenom. **19**, 231 (1980).
[13]A. P. Hitchcock, S. Beaulieu, T. Steel, J. Stöhr, and F. Sette, J. Chem. Phys. **80**, 3927 (1984).
[14]J. A. Horsley, J. Stöhr, A. P. Hitchcock, D. C. Newbury, A. L. Johnson, and F. Sette, J. Chem. Phys. **83**, 6099 (1985).
[15]A. N. Nesmeyanov and E. J. Kahn, Ber. Dtsch. Chem. Ges. **67B**, 370 (1934); A. I. Mashentsev, J. Gen. Chem. (USSR) **16**, 203 (1946).
[16]H. W. Morgan, P. A. Staats, and J. H. Goldstein, J. Chem. Phys. **25**, 337 (1956).
[17]W. Waring, Chem. Rev. **51**, 171 (1952).
[18]R. D. Leapman, L. A. Grunze, P. L. Fejes, and J. Silcox, in *EXAFS Spectroscopy, Techniques, and Applications*, edited by B. K. Teo and D. C. Joy (Plenum, New York, 1981), p. 217.
[19]M. Inokuti, Rev. Mod. Phys. **43**, 297 (1971).
[20]G. Doolan and D. Liberman, Total Absorption of Neutral Atoms, ab initio calculations (Lawrence Livermore Labs, 1986) unpublished.
[21]R. B. Kay, Ph. E. Van der Leeuw, and M. J. Van der Wiel, J. Phys. B **10**, 2513 (1977).
[22]R. McLaren, S. A. Clark, I. Ishii, and A. P. Hitchcock, Phys. Rev. A (submitted).
[23]G. C. King, M. Tronc, F. H. Read, and R. C. Bradford, J. Phys. B **10**, 2479 (1977); A. P. Hitchcock and C. E. Brion, Chem. Phys. **33**, 55 (1978); R. N. S. Sodhi and C. E. Brion, J. Electron Spectrosc. **37**, 97 (1985).
[24]W. L. Jolly, K. D. Bomben, and C. J. Eyermann, At. Data Nucl. Data Tables **31**, 433 (1984).
[25]I. Ishii, R. McLaren, A. P. Hitchcock, and M. B. Robin (manuscript in preparation).
[26]A. P. Hitchcock, P. Fischer, A. Gedanken, and M. B. Robin, J. Phys. Chem. (in press).
[27]S. P. McGlynn, L. G. Vanquickenborne, M. Kinoshita, and D. G. Carroll, *Introduction to Applied Quantum Chemistry* (Holt, Rineholt, and Winston, New York, 1972), p. 237.
[28]T. Ha and L. Keller, J. Mol. Struct. **27**, 225 (1975).
[29]J. L. Dehmer, J. Chem. Phys. **56**, 4496 (1972).
[30]D. A. Outka, J. Stöhr, R. J. Madix, H. H. Rotermund, B. Hermsmeier, and J. Solomon, Surf. Sci. (in press).
[31]H. Basch, M. B. Robin, and N. A. Kuebler, J. Chem. Phys. **49**, 5007 (1968); *ibid.* **47**, 1201 (1967).
[32]R. R. Hart and M. B. Robin, Theor. Chim. Acta **3**, 375 (1965).
[33]M. B. Robin, R. R. Hart, and N. A. Kuebler, J. Chem. Phys. **44**, 1803 (1966).
[34]W. L. Jorgensen and L. Salem, *The Organic Chemist's Book of Orbitals* (Academic, New York, 1973).
[35]*Structure Data of Free Polyatomic Molecules*, edited by Landolt–Bornstein, New Series II (Springer, Berlin, 1976), Vol. 7.
[36]A. P. Hitchcock and I. Ishii, J. Electron Spectrosc. **42**, 11 (1987).
[37]G. R. Wight and C. E. Brion, J. Electron Spectrosc. **3**, 191 (1974).